Electronic supplementary information for

Light-mediated the interface interaction of commercial graphene oxide in natural surface water: Photo-transform, microbial diversity, and metabolism

Yang Gao, [a] Li Chen, [a] Peihuan Wen, [a] Letao Zhou, [a] Shaohu Ouyang, [b,] * Wenjing Xue, [c] Wei Zhang, [a] Lean Zhou, [a] Jinting Wang, [a] and Shiquan Sun [a]

[a] *School of Hydraulic and Environmental Engineering, Changsha University of Science and Technology, Changsha 410114, China*

[b] *College of Environmental Science and Engineering, Nankai University, Tianjin 300350, China*

[c] *College of Environmental Science and Engineering, Yangzhou University, Yangzhou, 225009, China*

*Corresponding author: Shaohu Ouyang (ouyangshaohu@nankai.edu.cn).

The ESI contains 39 pages with 19 Figures and 11 Tables.

List of Supplemental Figures

List of Supplemental Tables

Natural surface waters

The natural surface water (depth, 0.5 m) was collected from Xiangjiang River (♦ (112.97, 28.15), Hunan province, China) by organic glass hydrophore and collected in polyethylene containers. Xiangjiang River is the longest river of the Hunan province (Span: 948 km, Total basin area: 94721 km^2). The Xiangjiang River basin is the most densely populated area with the highest urbanization level and the most developed economy, society, and culture in Hunan Province. Before use, all the instruments and vessels used in the sampling were cleaned and treated with 10% nitric acid solution and Milli Q water (UPR-II-10TNZ, China) (18.2 MΩ · cm). The natural surface water samples were stored around the ice bags (kept in the dark) during sampling and delivery and then immediately transported to the laboratory for further analysis.

Metabolite extraction

500 mg solid samples were accurately weighed, and the metabolites were extracted using a 400 μL methanol: water (4:1, v/v) solution with 0.02 mg/mL L-2-chlorophenylalanin as internal standard. The mixture was allowed to settle at -10 ºC and treated by High throughput tissue crusher Wonbio-96c (Shanghai Wanbo Biotechnology Co., LTD) at 50 Hz for 6 min, then followed by ultrasound at 40 kHz for 30 min at 5 ºC. The samples were placed at -20 ºC for 30 min to precipitate proteins. After centrifugation at 13000 g at 4 ºC for 15 min, the supernatant was carefully transferred to sample vials for LC-MS/MS analysis.

UHPLC-MS/MS analysis

The instrument platform for this LC-MS analysis is the UHPLC-Q Exactive HF-X

system of Thermo Fisher Scientific. 2 μL of sample was separated by HSS T3 column (100 mm × 2.1 mm i.d., 1.8 μm) and then entered into mass spectrometry detection. The mobile phases consisted of 0.1% formic acid in water: Acetonitrile (95:5, v/v) (solvent A) and 0.1% formic acid in acetonitrile: Isopropanol: water (47.5:47.5:5, v/v) (solvent B). The solvent gradient changed according to the following conditions: from 0 to 3.5 min, 0% B to 24.5% B (0.4 mL/min); from 3.5 to 5 min, 24.5% B to 65% B (0.4 mL/min); from 5 to 5.5 min, 65% B to 100% B (0.4 mL/min); from 5.5to 7.4 min, 100% B to 100% B (0.4 mL/min to 0.6 mL/min); from 7.4 to 7.6 min, 100% B to 51.5% B (0.6 mL/min); from 7.6 to 7.8 min, 51.5% B to 0% B (0.6 mL/min to 0.5 mL/min); from 7.8 to 9 min, 0% B to 0% B (0.5 mL/min to 0.4 mL/min); from 9 to 10 min, 0% B to 0% B (0.4 mL/min) for equilibrating the systems. The sample injection volume was 2 μL and the flow rate was set to 0.4 mL/min. The column temperature was maintained at 40 ºC. During the period of analysis, all these samples were stored at 4 ºC.

The mass spectrometric data was collected using a Thermo UHPLC -Q Exactive HF-X Mass Spectrometer equipped with an electrospray ionization (ESI) source operating in either positive or negative ion mode. The optimal conditions were set as follows: heater temperature, 425 ºC; Capillary temperature, 325 ºC; sheath gas flow rate, 50 arb; Aux gas flow rate, 13 arb; ion-spray voltage floating (ISVF), -3500V in negative mode and 3500V in positive mode, respectively; Normalized collision energy, 20-40-60V rolling for MS/MS. Full MS resolution was 60000, and MS/MS resolution was 7500. Data acquisition was performed with the Data Dependent Acquisition (DDA) mode.

The detection was carried out over a mass range of 70-1050 m/z.

Data preprocessing and annotation

After the mass spectrometry detection is completed, the raw data of LC/MS is preprocessed by Progenesis QI (Waters Corporation, Milford, USA) software, and a three-dimensional data matrix in CSV format is exported. The information in this three-dimensional matrix includes: sample information, metabolite name, and mass spectral response intensity. Internal standard peaks, as well as any known false positive peaks (including noise, column bleed, and derivatized reagent peaks), were removed from the data matrix, deredundant, and peak pooled. At the same time, the metabolites were searched and identified, and the main database was the HMDB (http://www.hmdb.ca/), Metlin (https://metlin.scripps.edu/), and Majorbio Database.

The data after the database search is uploaded to the Majorbio cloud platform (https://cloud.majorbio.com) for data analysis. Metabolic features detected at least 80 % in any set of samples were retained. After filtering, minimum metabolite values were imputed for specific samples in which the metabolite levels fell below the lower limit of quantitation and each Metabolic feature was normalized by sum. To reduce the errors caused by sample preparation and instrument instability, the response intensity of the sample mass spectrum peaks was normalized by the sum normalization method, and the normalized data matrix was obtained. At the same time, variables with relative standard deviation (RSD) > 30% of QC samples were removed, and log10 logarithmization was performed to obtain the final data matrix for subsequent analysis.

Differential metabolites analysis

Perform variance analysis on the matrix file after data preprocessing. The R package ropls (Version 1.6.2) performed principal component analysis (PCA) and orthogonal least partial squares discriminant analysis (OPLS-DA) and used 7-cycle interactive validation to evaluate the stability of the model. In addition, the student's t-test and fold difference analysis were performed. The selection of significantly different metabolites was determined based on the Variable importance in the projection (VIP) obtained by the OPLS-DA model and the p-value of the student's t-test, and the metabolites with VIP>1, $p<0.05$ were significantly different. A total of 332 (pos) and 268 (neg) differential metabolites were screened.

Differential metabolites among two groups were summarized, and mapped into their biochemical pathways through metabolic enrichment and pathway analysis based on a database search (KEGG, http://www. genome.jp/kegg/). These metabolites can be classified according to the pathways they are involved in or the functions they perform. Enrichment analysis was usually to analyze a group of metabolites in a function node whether appears or not. The principle was that the annotation analysis of a single metabolite develops into an annotation analysis of a group of metabolites. scipy. stats (Python packages) (https://docs.scipy.org/doc/scipy/) was exploited to identify statistically significantly enriched pathways using Fisher's exact test.

Pearson correlation coefficient (PCC) analyze

PCC was used to analyze the similarity and correlation between samples. As shown in Figure 6B (dotted box 1), the average PCC between XJW0 and XJW48 is 0.86, which implies that the two groups are highly positively correlated. In contrast, the dotted box

2 shows the control group (XJW: XJW0 and XJW48) and the exposed group (XJW+GO2, XJW+GO5, XJW+GO+UV, and XJW+UV) were not correlated strongly and were at a low level. The dotted box 3 shows the control group XJW+GO2 and XJW+GO5 were not correlated strongly with XJW0. While dotted box 4 (XJW+UV and XJW+GO+UV) shows a weaker correlation than dotted box 3 (XJW+GO). What is more, dotted box 5 (XJW+UV) showed a weak correlation to the groups without UV exposure, indicating the different effects between GO and UV exposure. The dotted box 6 (XJW+GO+UV) shows a strong correlation with XJW+UV and XJW+GO, indicating the combined effects of GO and UV exposure. Those results were approximately consistent with PCA analysis distinctions in the metabolic profiles (Figure 6A).

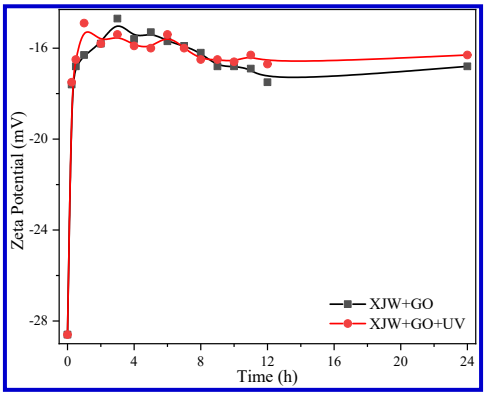

Figure S1. The zeta potential of CGO in XJW without/with UV exposure as a function of time (CGO: 20 mg/L).

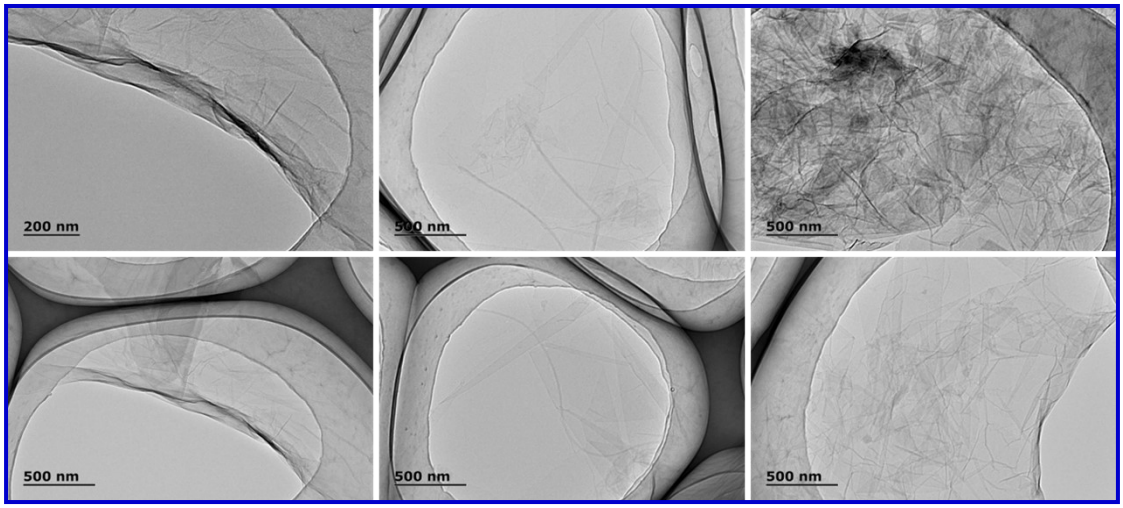

Figure S2. TEM images of CGO +XJW (CGO: 20 mg/L).

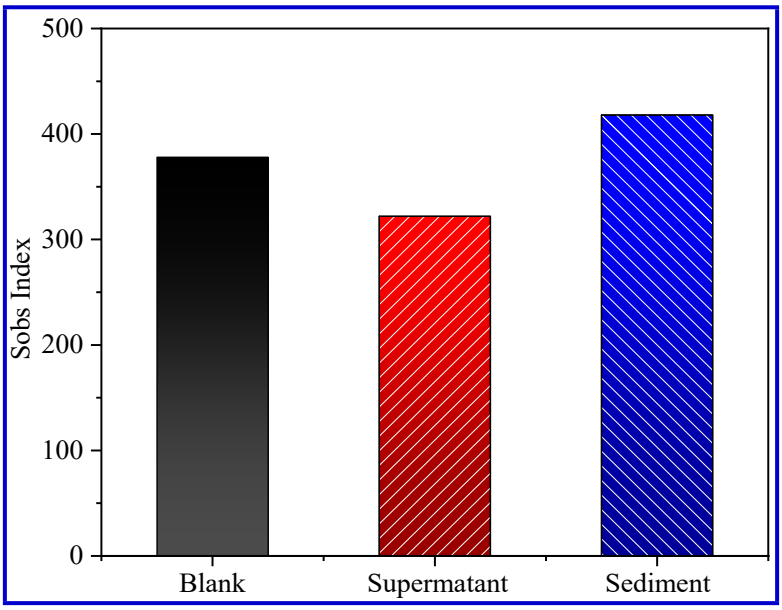

Figure S3. Comparison of Sobs index during the three groups.

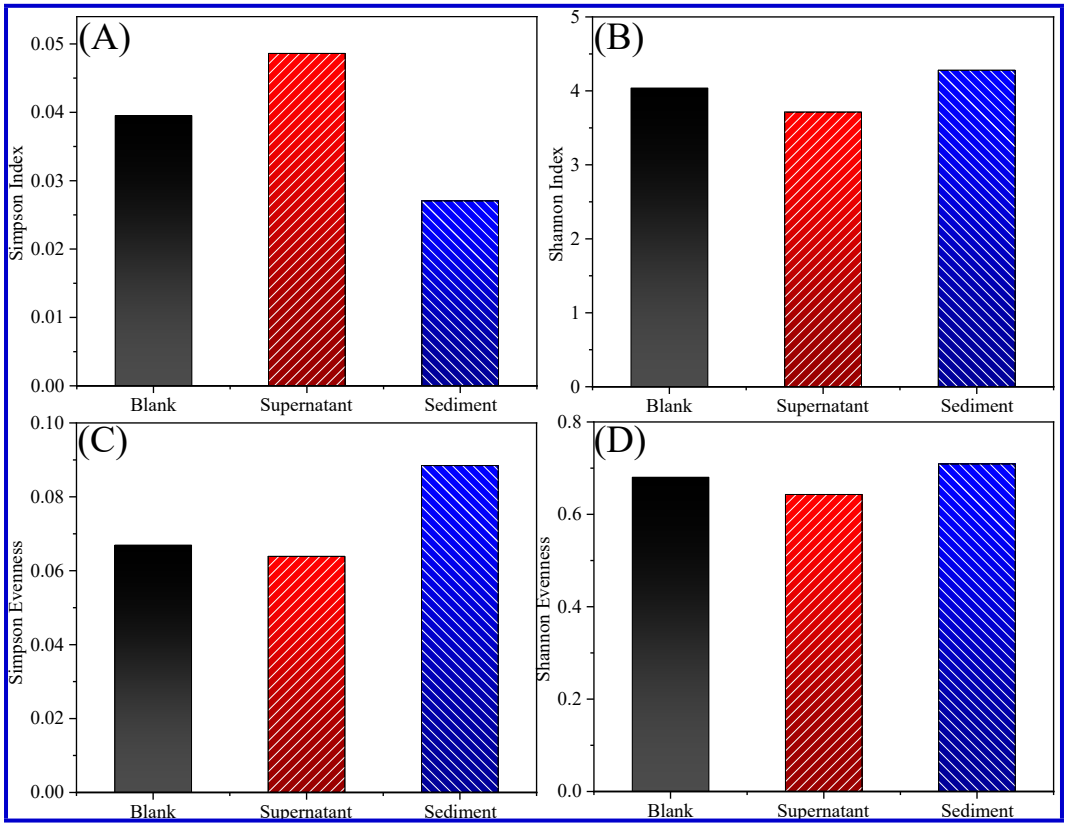

Figure S4. The α diversity comparison of the three groups at the species level. Shannon index (A), Simpson index (B), Shannon evenness (C), and Simpson evenness (D).

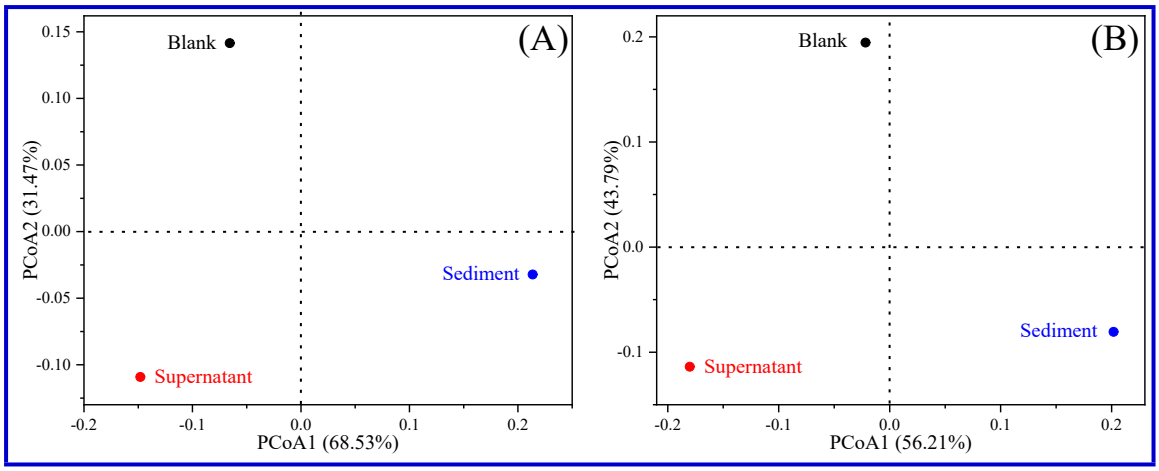

Figure S5. PCoA plots of Bray−Curtis distances at the genus (A) and species (B) levels.

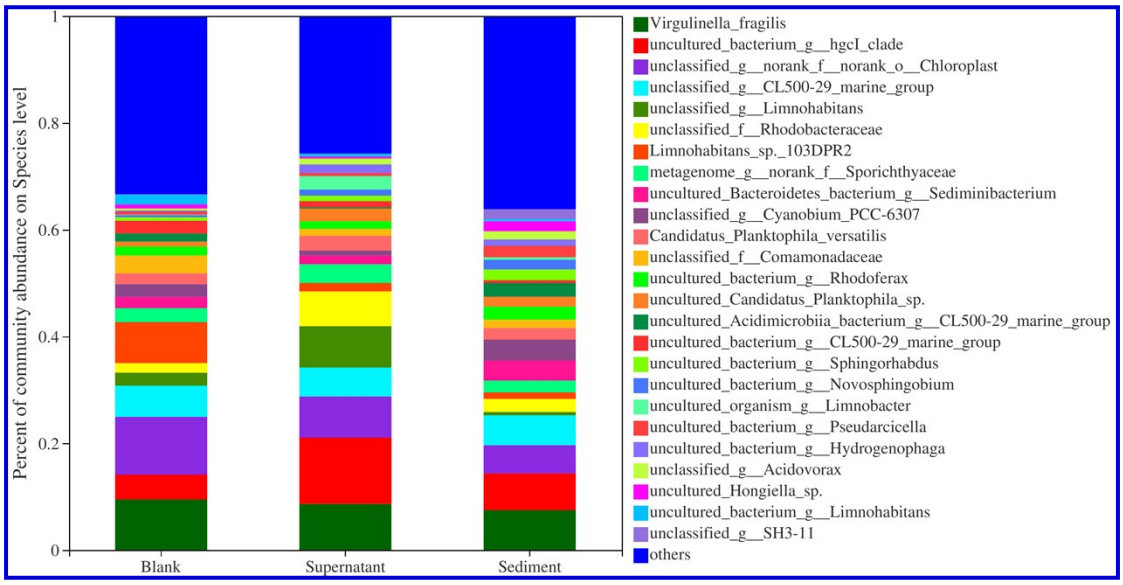

Figure S6. Relative abundance of the major bacteria species among different groups.

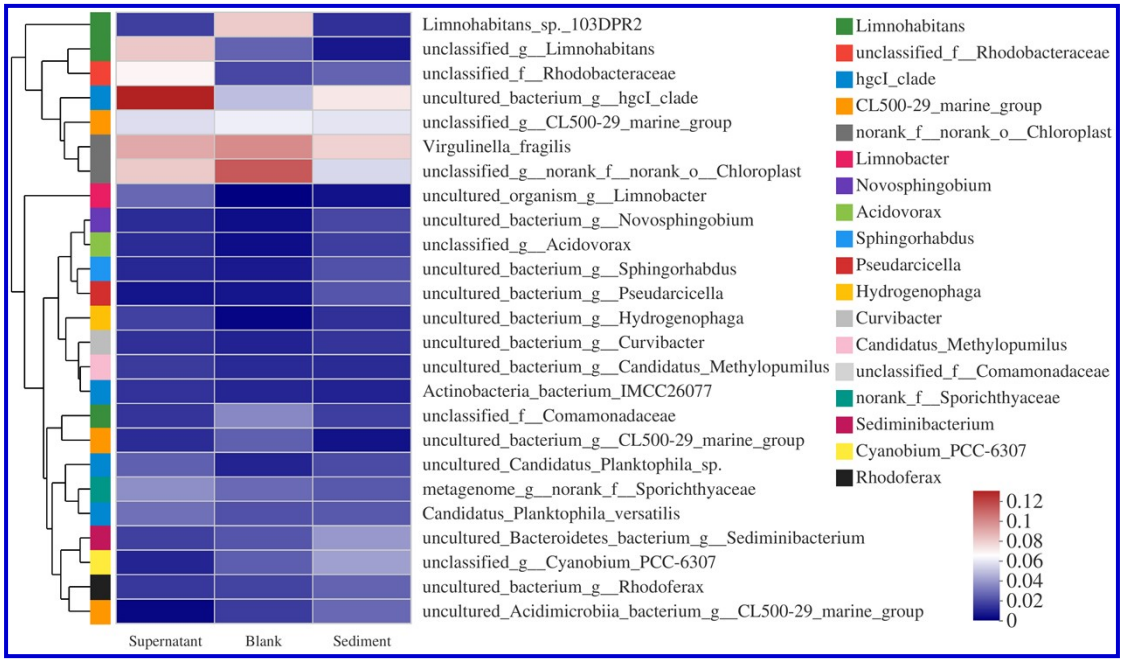

Figure S7. The microbial community heatmap analysis on species level.

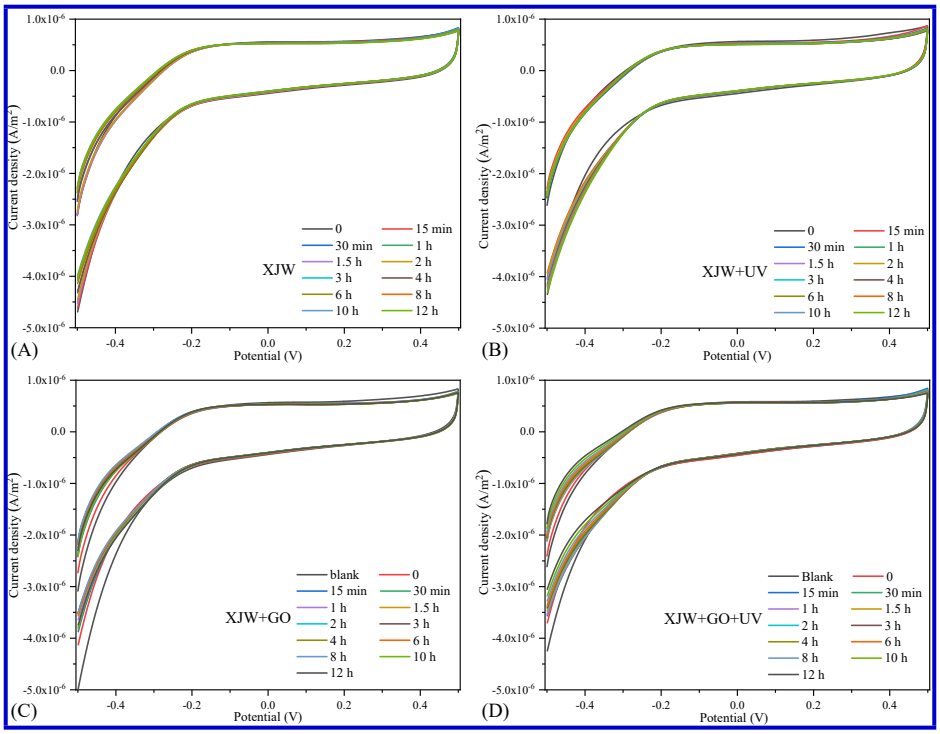

Figure S8. The cyclic voltammetry curves of different aqueous solution systems. (A) XJW, (B) XJW+UV, (C) XJW+GO and (D) XJW+GO+UV.

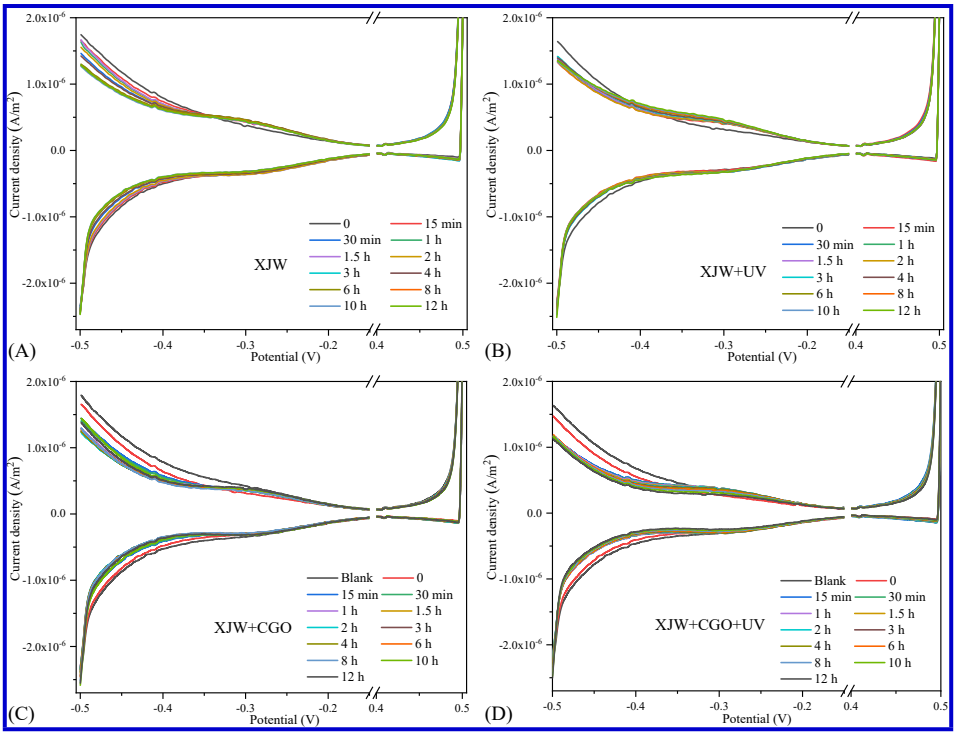

Figure S9. The first-order derivative of the cyclic voltammetry curves of different aqueous solution systems. (A) XJW, (B) XJW+UV, (C) XJW+GO and (D) XJW+GO+UV.

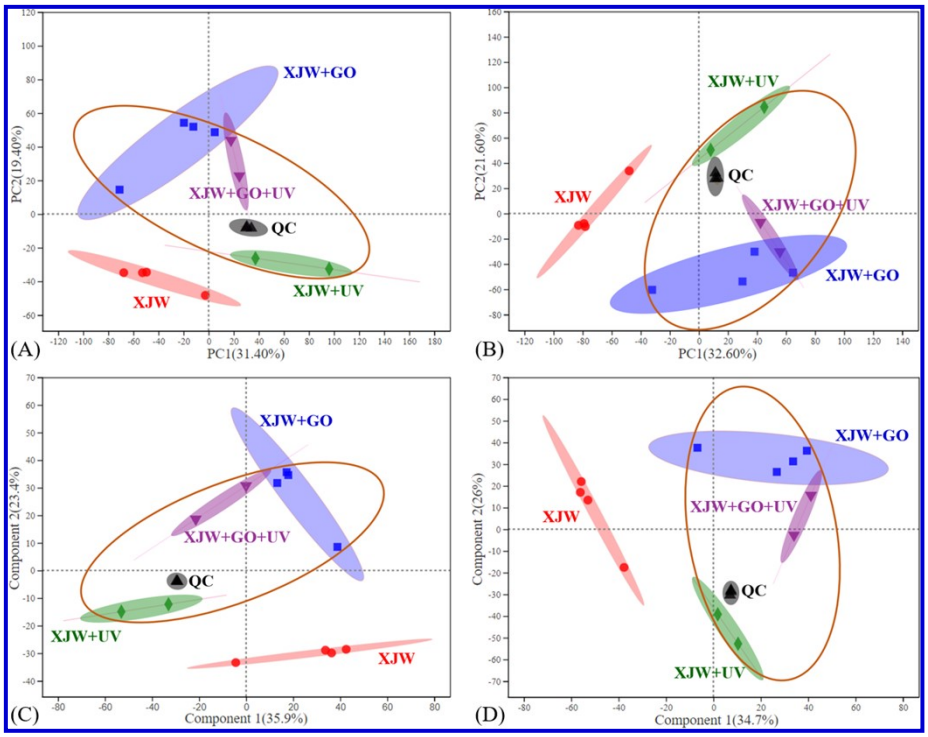

Figure S10. Integration of polar metabolites and transcript revealed toxicity induced by CGO. The PCA score plot of metabolites (A) pos, (B) neg; The PLS-DA score plot of metabolites (C) pos, (D) neg.

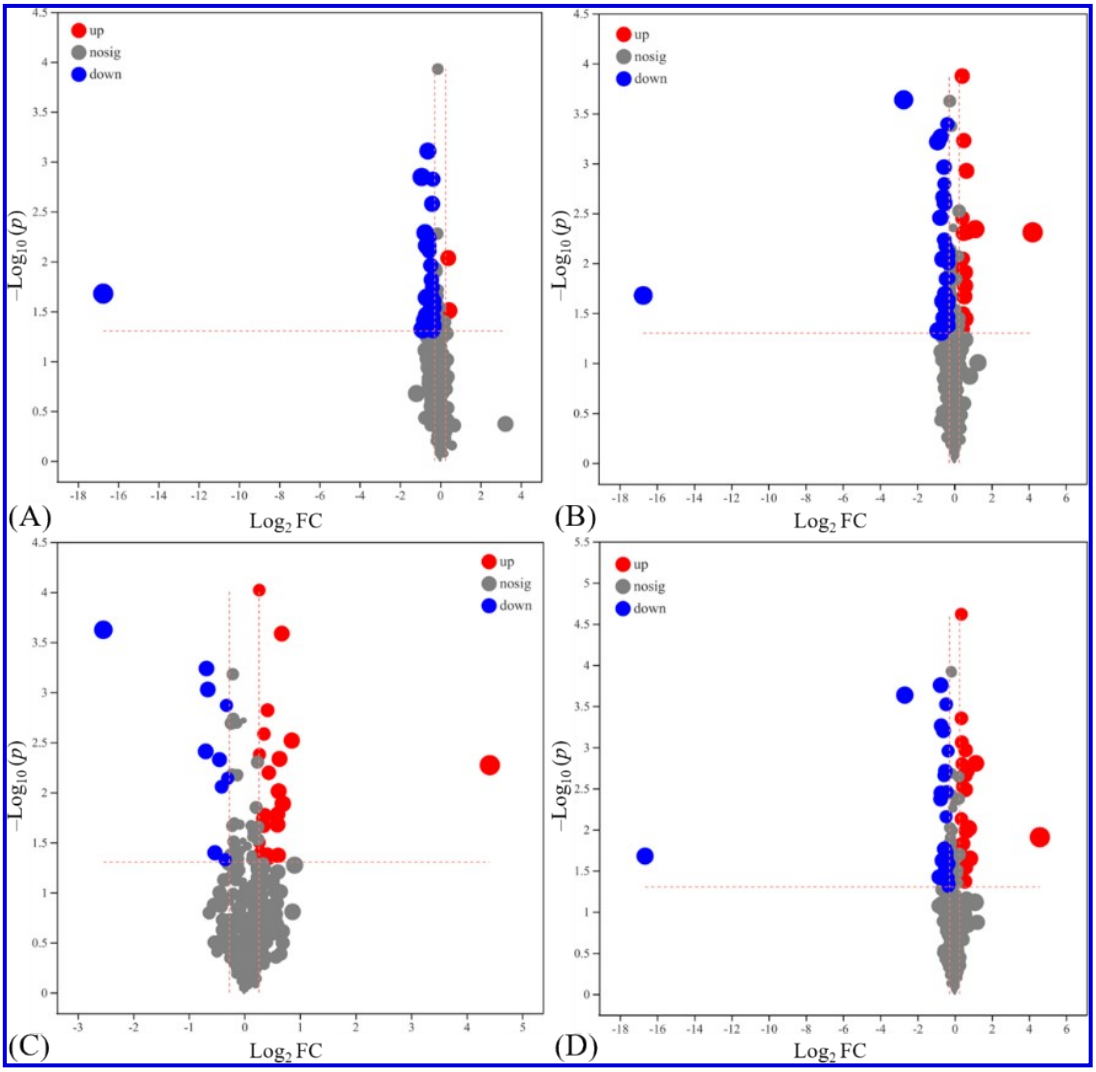

Figure S11. The volcanic map of differential metabolites (pos+neg) of (A) GO2-XJW48, (B) GO5-XJW48, (C) UV-XJW48, and (D) GOUV-XJW48. (The red and blue dots were considered to indicate significantly upregulated and downregulated metabolites, respectively. Metabolites shown in gray dots were not significantly changed or those were not measured.)

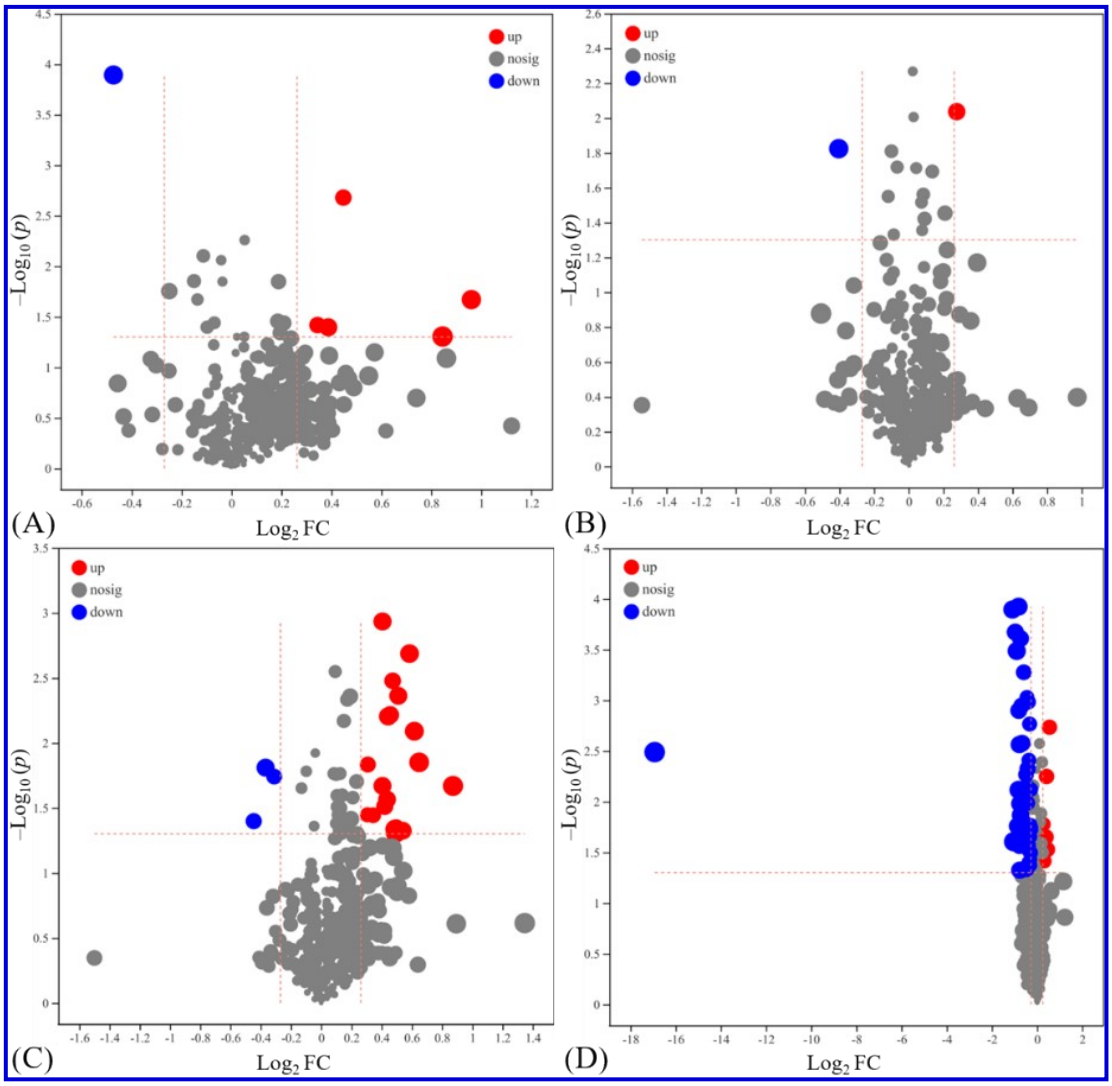

Figure S12. The volcanic map of differential metabolites (pos+neg) of (A) XJW48-XJW0, (B) GO5-GO2, (C) GOUV-GO, and (D) GOUV-UV. (The red and blue dots were considered to indicate significantly upregulated and downregulated metabolites, respectively. Metabolites shown in gray dots were not significantly changed or those were not measured.)

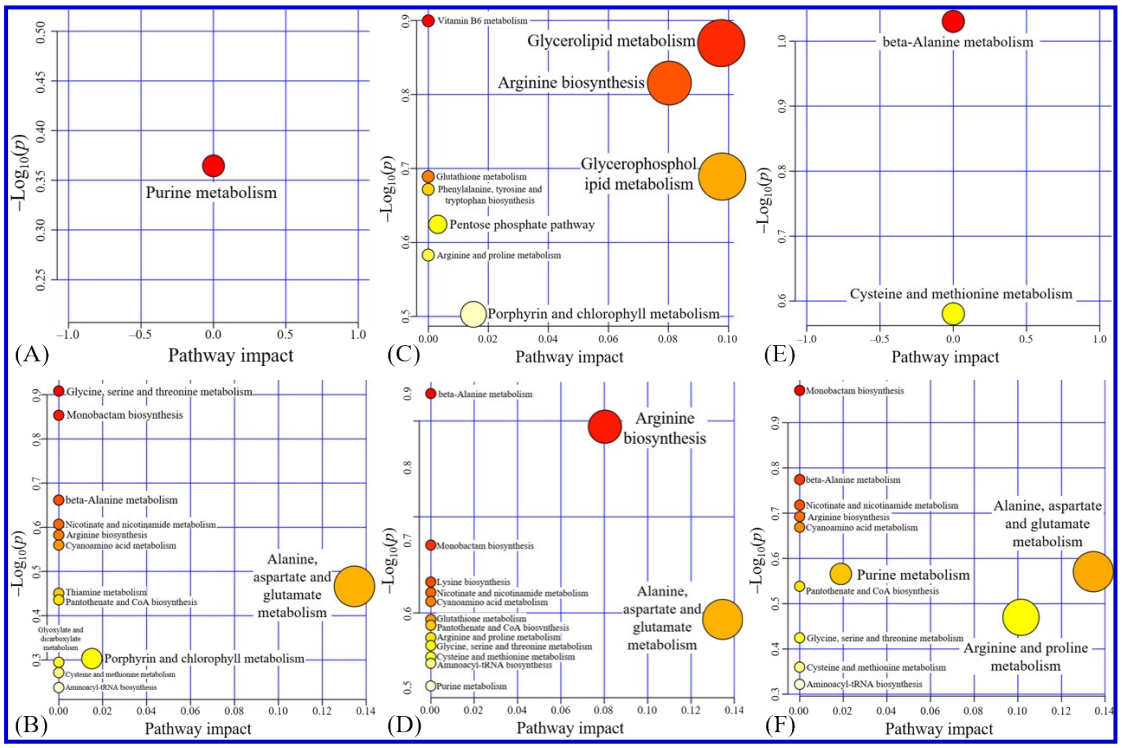

Figure S13. Significantly disturbed metabolic pathways in (A) GO2-XJW48; (B) GO5-XJW48; (C) UV-XJW48; (D) GOUV-XJW48; (E) GOUV-GO; (F) GOUV-UV.

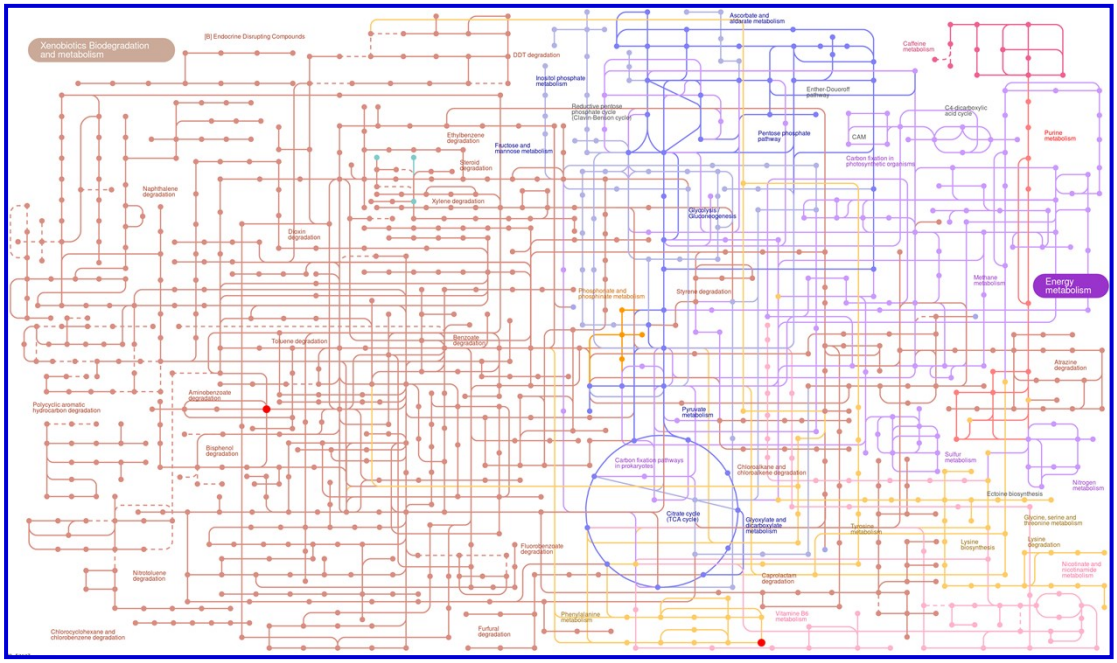

Figure S14. The microbial metabolism pathways of GO2-XJW48 were constructed based on the iPath 3 pathway database. Metabolites with an arresting red color are highlighted based on the comparisons of the treatment groups with the control.

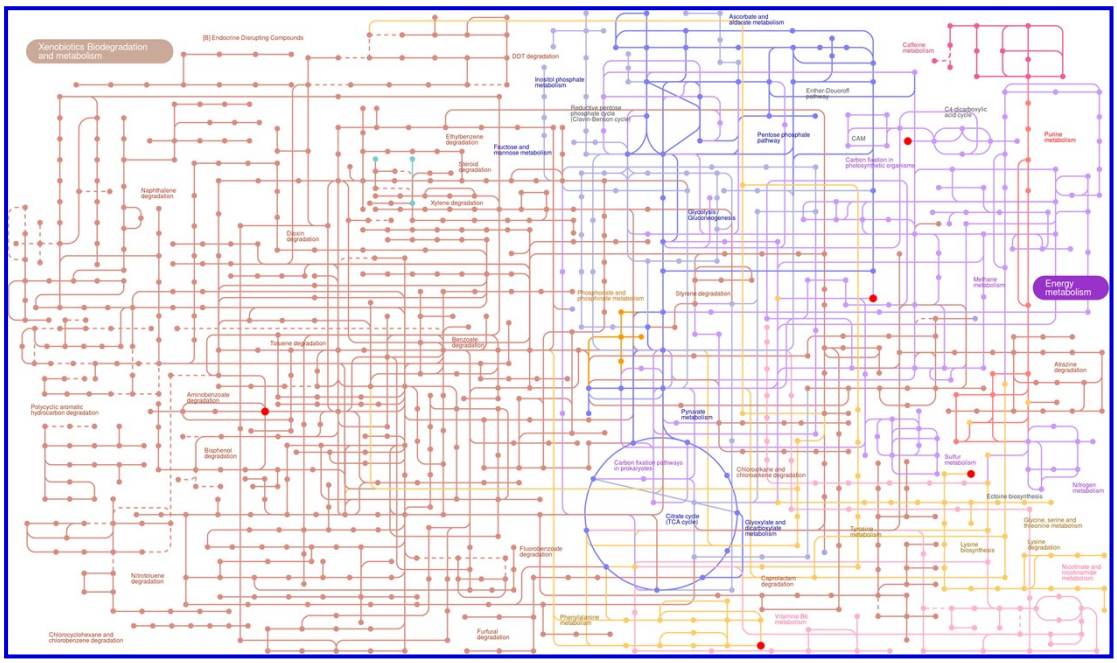

Figure S15. The microbial metabolism pathways of GO5-XJW48 were constructed based on the iPath 3 pathway database. Metabolites with an arresting red color are highlighted based on the comparisons of the treatment groups with the control.

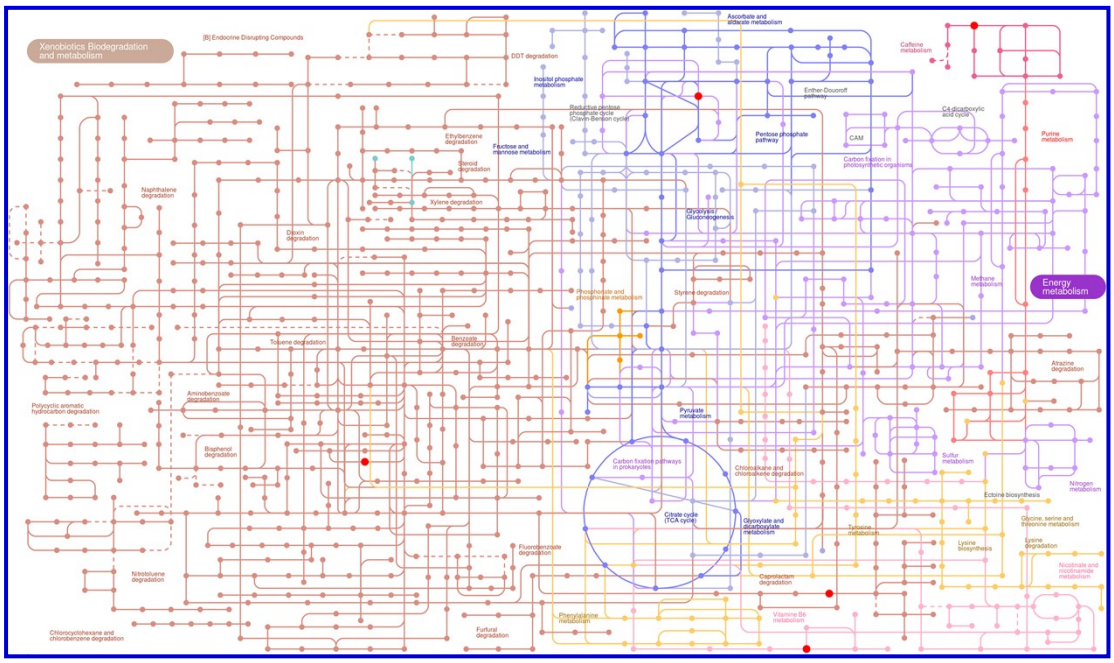

Figure S16. The microbial metabolism pathways of UV-XJW48 were constructed based on the iPath 3 pathway database. Metabolites with an arresting red color are highlighted based on the comparisons of the treatment groups with the control.

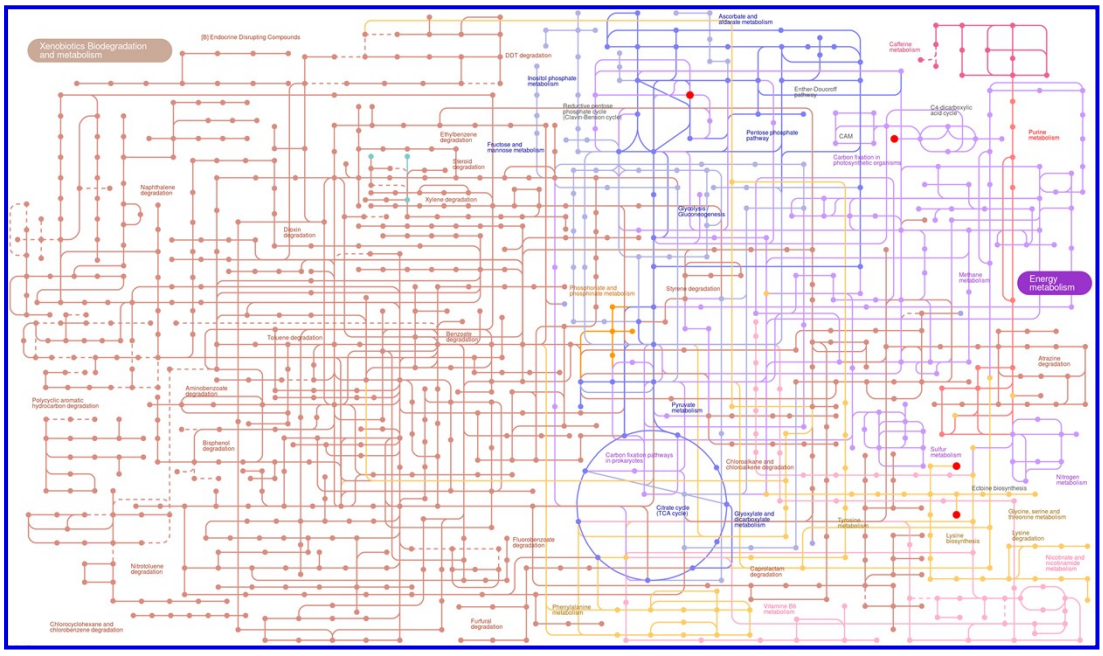

Figure S17. The microbial metabolism pathways of GOUV-XJW48 were constructed based on the iPath 3 pathway database. Metabolites with an arresting red color are highlighted based on the comparisons of the treatment groups with the control.

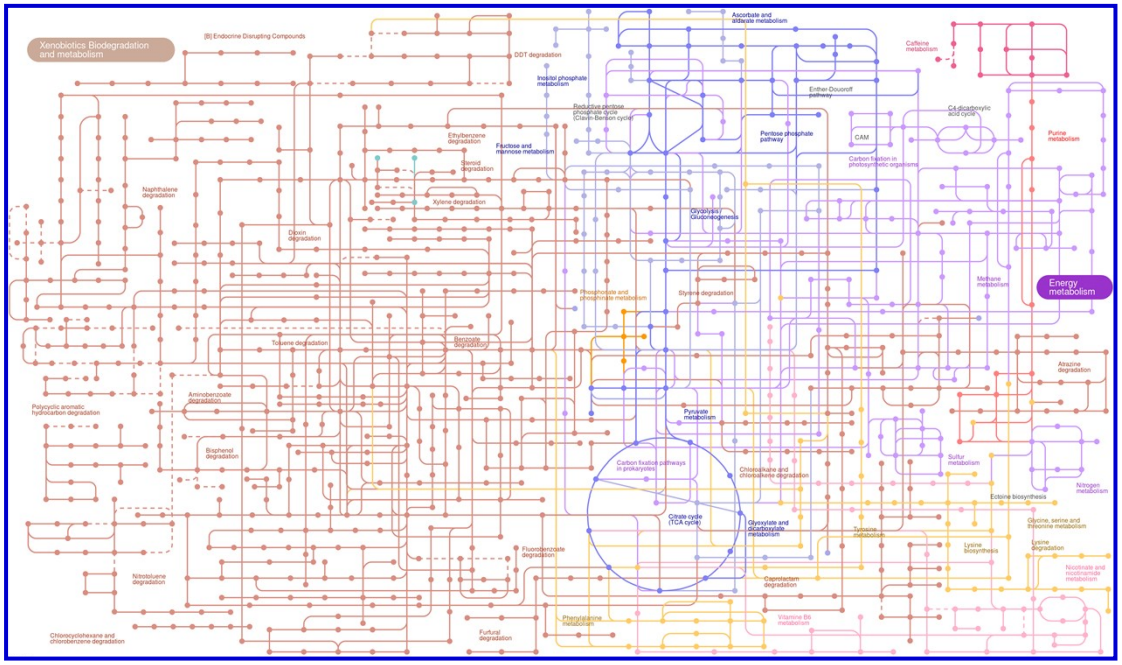

Figure S18. The microbial metabolism pathways of GO5-GO2 were constructed based on the iPath 3 pathway database. Metabolites with an arresting red color are highlighted based on the comparisons of the treatment groups with the control.

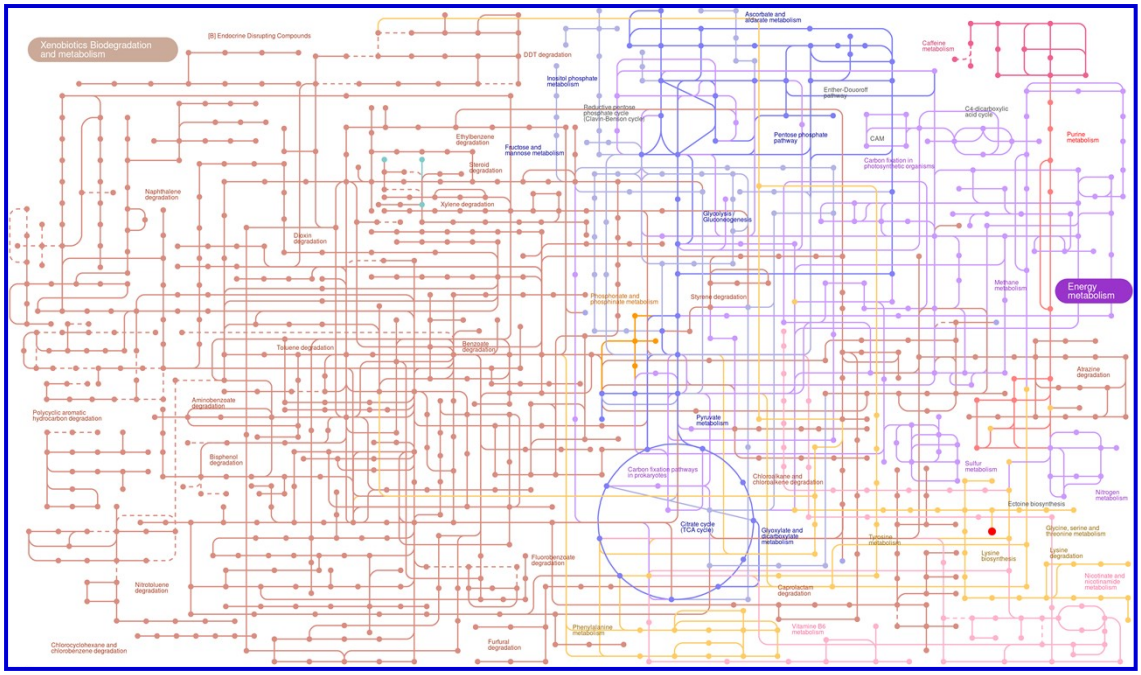

Figure S19. The microbial metabolism pathways of GOUV-GO2 were constructed based on the iPath 3 pathway database. Metabolites with arresting red color are highlighted based on the comparisons of the treatment groups with the control

Table S1. Technical data of the commercial GO purchased from TIMESNANO[a]

Name	Purity	layers	Thickness	Diameter	Color	Selling State
GO Gel	> 99 wt %	< 3	0.55−1.2 nm	0.5−3 μm	Brown	Water Gel

[a]Http://www.timesnano.com

Table S2. Physicochemical properties of the XJW.

Water type	pH	TOC (mg/L)	K (mM)	Na (mM)	Mg (mM)	Ca (mM)	Cond (ms/cm)
XJW	8.3	1.91	0.11	0.50	0.22	0.92	0.312

Table S3. The Raman peak analysis of D-bond and G-bond by Gaussian.

Sample	Peak	P (cm^{-1})	H	FWHM	Area	I_D/I_G
CGO+XJW	D-bond	1362.41	3359.95	161.32	576984.77	1.25
	G-bond	1583.78	3870.89	111.95	461320.08	
CGO+XJW +UV	D-bond	1361.40	3331.36	172.20	607099.91	1.42
	G-bond	1587.42	3806.35	105.86	428925.04	

Table S4. XPS data of the C 1s and O 1s of the CGO, CGO+XJW, and CGO+XJW+UV.

Sample	C (eV)			O (eV)		
	C=C	C−O	C=O	C=O	O−H	C−O−C
CGO	284.35	286.31	288.03	531.16	532.16	532.92
CGO+XJW	284.11	286.03	287.57	530.72	531.88	532.72
CGO+XJW+UV	283.86	285.70	287.55	530.81	531.88	532.79
Sample	C (Area)			O (Area)		
	C=C	C−O	C=O	C=O	O−H	C−O−C
CGO	135702.9	118929.2	23101.0	93100.4	158724.4	97199.9
CGO+XJW	200962.4	109231.9	32210.1	92937.5	136467.3	98194.6
CGO+XJW+UV	231307.0	84357.4	29884.3	145634.1	98174.8	63535.9

Table S5. The relative abundance (%) of major bacterial phyla and genera in Sediment (SM), Supernatant (SN), and Blank (BL).

Phylum	Proteobacteria	Actinobacteriota	Cyanobacteria	Bacteroidota	Others	Verrucomicrobiota	Planctomycetota
SM	34	25	17	16	2.6	2.7	1.4
SN	43	32	19	4.6	1.7	0.19	0.17
BL	38	25	24	8.9	3.5	0.44	0.69
Genus	Others	Norank_f_norank _o_Chloroplast	Hgcl_clade	CL500-29_ Marine_group	Limnoha bitans	Unclassified_f_ Rhodobacteraceae	Cyanobium_PCC -6307
SM	57	13	12	9.1	2.2	2.5	4.1
SN	38	18	20	6.9	9.9	6.5	0.97
BL	43	22	9.5	10	12	1.8	2.4

Table S6. The comparison of the relative abundance (%) of major bacterial phyla and genera among Sediment (SM), Supernatant (SN), and Blank (BL).

Phylum	SM	SN	BL	**Genus**	SM	SN	BL
Proteobacteria	30	37	33	Others	41	28	31
Actinobacteriota	31	39	30	Norank_f_norank_o_Chloroplast	25	34	41
Cyanobacteria	29	31	40	Hgcl_clade	29	48	22
Bacteroidota	55	15	30	CL500-29_Marine_group	35	26	39
Others	34	22	44	Limnohabitans	9.3	41	50
Verrucomicrobiota	81	5.7	13	Unclassified_f_Rhodobacteraceae	23	60	17
Planctomycetota	63	7.6	30	Cyanobium_PCC-6307	55	13	32

Table S7. The statistical table of differential metabolism in different groups. A fold change (FC) > 1.2 and $p < 0.05$ or fold change < 0.83 and $p < 0.05$ were considered to indicate significantly upregulated and downregulated metabolites, respectively.

Mode	Total number	GO2-XJW48	GO5-XJW48	UV-XJW48	GOUV-XJW48
pos	905(45)	236(13)	563(26)	307(14)	499(30)
neg	1706(59)	480(21)	1075(32)	561(18)	1052(30)
Total	2611(104)	716(34)	1638(58)	868(32)	1551(60)
Mode	XJW48-XJW0	GO5-GO2	GOUV-GO	GOUV-UV	
pos	29(3)	87(0)	160(11)	369(30)	
neg	98(3)	59(2)	147(11)	604(26)	
Total	127(6)	146(2)	307(22)	973(56)	

Table S8. The variable importance in the projection (VIP), Fold change (FC), *p-value*, and false discovery rate (FDR) value in metabolites abundance of GO2-XJW48. The FC > 1.2 and $p < 0.05$ or FC < 0.83 and $p < 0.05$ were considered to indicate significantly upregulated and downregulated metabolites, respectively.

Mode ID	Metabolite	VIP (OPLS-DA)	VIP (PLS-DA)	FC	P_value	FDR
neg_7660	Seryltryptophan	3.1456	2.9928	0	0.02104	0.3956
pos_851	Asp-Val-OH	2.7009	2.6046	0.5475	0.04789	0.6552
pos_7859	Vaccinoside	2.6406	2.548	0.6378	0.006953	0.4856
neg_9680	Fructosamine	2.6222	2.5362	0.5285	0.001425	0.3731
pos_904	Lumichrome	2.5534	2.4614	0.63	0.02308	0.6053
pos_7175	Succinoadenosine	2.5316	2.4406	0.5902	0.03927	0.6443
neg_4274	Hexadecanedioic acid mono-L-carnitine ester	2.4511	2.3173	0.6299	0.03463	0.4127
neg_3893	Butyl (S)-3-hydroxybutyrate glucoside	2.3617	2.2628	0.5935	0.00517	0.3731
pos_6460	5-Hydroxysulfamethoxazole	2.3499	2.2651	0.6733	0.03589	0.6408
neg_1939	Threoninyl-Gamma-glutamate	2.3056	2.1708	0.6364	0.04483	0.432
pos_5791	Tangeritin	2.3	2.2302	0.7242	0.03903	0.6443
pos_6936	5-Hydroxy-L-tryptophan	2.2727	2.1963	0.6526	0.0007831	0.3686
pos_3933	Austalide L	2.2553	2.212	1.3475	0.03113	0.6397
pos_6937	1H-Indole-3-acetamide	2.1717	2.0834	0.6916	0.03208	0.6397
pos_3542	(1R*,2R*,4R*,8S*)-p-Menthane-1,2,8,9-tetrol 9-glucoside	2.0322	1.9669	0.7567	0.002649	0.3913
neg_5984	PE(15:0/0:0)	2.0296	2.0053	0.7162	0.04223	0.4271
neg_4719	PG(16:0/0:0)[U]	2.0251	1.9577	0.7344	0.02233	0.3975
pos_3664	(S)-10,16-Dihydroxyhexadecanoic acid	2.0001	1.9323	1.3183	0.009258	0.5331
neg_2875	Tyrosyl-Proline	1.9479	1.8411	0.709	0.03127	0.4082
neg_7629	Gamma-Glutamylphenylalanine	1.9416	1.8607	0.669	0.005801	0.3731

pos_3393	6-{[3-(2,4-dihydroxyphenyl)propanoyl]oxy}-3,4,5-trihydroxyoxane-2-carboxylic acid	1.9236	1.8539	0.8001	0.04368	0.6552
neg_4371	Corchorifatty acid A	1.8923	1.8229	0.738	0.01531	0.3774
neg_4782	Gamma-Eudesmol rhamnoside	1.8299	1.7785	0.7219	0.01097	0.3731
neg_8440	Xanthopterin	1.8134	1.7072	0.6796	0.0432	0.4271
pos_3761	Monotropein	1.7957	1.7338	0.7772	0.0015	0.3686
neg_2788	Valyl-Proline	1.7672	1.6812	0.7706	0.04957	0.4424
neg_9003	A-L-Arabinofuranosyl-(1->2)-[a-D-mannopyranosyl-(1->6)]-D-mannose	1.7276	1.6524	0.762	0.01817	0.3775
neg_5933	PE(16:0/0:0)	1.7174	1.6245	0.8142	0.02903	0.4027
neg_7015	S-Nitrosoglutathione	1.7009	1.6916	0.8095	0.02484	0.3975
neg_7164	Indolelactic acid	1.6767	1.6202	0.6837	0.007912	0.3731
neg_2295	6-({3,5-dihydroxy-2-methyl-6-[(3,4,5,6-tetrahydroxyoxan-2-yl)methoxy]oxan-4-yl}oxy)-3,4,5-trihydroxyoxane-2-carboxylic acid	1.6126	1.5631	0.7981	0.03647	0.4165
neg_9122	ADP-ribose	1.5448	1.5136	0.7645	0.03379	0.4116
neg_6254	3b-Hydroxy-6b-methoxy-7(11)-eremophilen-12,8a-olide	1.5008	1.411	0.7813	0.04816	0.4413
neg_6156	(10Z,14E,16E)-10,14,16-Octadecatrien-12-ynoic acid	1.4014	1.319	0.8253	0.04581	0.433

Table S9. The variable importance in the projection (VIP), Fold change (FC), *p-value*, and false discovery rate (FDR) value in metabolites abundance of GO5-XJW48. The FC > 1.2 and $p < 0.05$ or FC < 0.83 and $p < 0.05$ were considered to indicate significantly upregulated and downregulated metabolites, respectively.

Mode ID	Metabolite	VIP (OPLS-DA)	VIP (PLS-DA)	FC	P_value	FDR
pos_2802	(15a,20R)-Dihydroxypregn-4-en-3-one 20-[glucosyl-(1->4)-6-acetyl-glucoside]	3.2377	3.2213	18.5772	0.004911	0.1331
neg_6907	2-{[hydroxy(4-methoxy-1-benzofuran-5-yl)methylidene]amino}acetic acid	2.8491	2.8489	0.1518	0.0002312	0.0299
neg_7660	Seryltryptophan	2.7576	2.7575	0	0.02104	0.1202
neg_3278	(6-carboxy-3,4,5-trihydroxyoxan-2-yl)[2-(3,4-dihydroxyphenyl)-3,5,6-trihydroxy-7H-chromen-7-ylidene]oxidanium	2.6233	2.6232	2.1916	0.00457	0.0498
pos_851	Asp-Val-OH	2.3928	2.38	0.5463	0.04747	0.2435
neg_9680	Fructosamine	2.3172	2.317	0.5365	0.0006096	0.04177
pos_7859	Vaccinoside	2.2796	2.2656	0.6524	0.009106	0.1729
pos_3664	(S)-10,16-Dihydroxyhexadecanoic acid	2.183	2.1745	1.5069	0.03603	0.2107
pos_5791	Tangeritin	2.178	2.1656	0.6902	0.024	0.1978
pos_7175	Succinoadenosine	2.1501	2.1371	0.6183	0.04938	0.247
neg_4274	Hexadecanedioic acid mono-L-carnitine ester	2.1259	2.1259	0.642	0.02404	0.1287
pos_904	Lumichrome	2.0983	2.0887	0.6718	0.04468	0.2356
neg_3893	Butyl (S)-3-hydroxybutyrate glucoside	2.0847	2.0845	0.5956	0.00351	0.04901
pos_6460	5-Hydroxysulfamethoxazole	2.0814	2.0699	0.6721	0.03532	0.2083
neg_7149	16,17-Dihydro-16a,17-dihydroxygibberellin A4 17-glucoside	2.0775	2.0775	1.4928	0.01683	0.1048
neg_6891	5'-Deoxy-5-fluorouridine	2.0518	2.0517	0.601	0.0005417	0.04115
neg_6844	5'-((Z)-Feruloyl) 3-(2'-methylarabinosylxylose)	2.017	2.0169	1.6494	0.004843	0.05184

neg_7153	3,4,5-trihydroxy-6-(2-methyl-3-phenylpropoxy) oxane-2-carboxylic acid	2.0144	2.0142	1.5716	0.001191	0.04901
pos_8202	5,7-dihydroxy-2-phenyl-8-(3,4,5-trihydroxyoxan-2-yl)-4H-chromen-4-one	2.0099	1.9986	1.4161	0.004993	0.1331
pos_3542	(1R*,2R*,4R*,8S*)-p-Menthane-1,2,8,9-tetrol 9-glucoside	1.9999	1.9889	0.6971	0.002508	0.09936
pos_7644	PELLETIERINE	1.9981	1.9875	1.4607	0.02154	0.1978
pos_6936	5-Hydroxy-L-tryptophan	1.9656	1.955	0.6642	0.00218	0.09272
neg_3848	Thiamine triphosphate	1.9296	1.9295	1.5011	0.01233	0.08906
pos_6631	4-AMINOETHYLBENZENESULFONYL FLUORIDE	1.9227	1.9122	0.682	0.001091	0.06865
pos_3274	Aloe emodin anthrone	1.8755	1.865	1.3441	0.0001338	0.03927
neg_5984	PE(15:0/0:0)	1.863	1.8626	0.702	0.02013	0.1175
neg_1774	L-Aspartic Acid	1.8624	1.8622	0.7097	0.03989	0.1708
neg_3846	Quercetagitrin	1.8523	1.8524	1.4446	0.01274	0.09071
pos_3933	Austalide L	1.8462	1.8381	1.3065	0.04593	0.2391
neg_7136	6-{[1,3-dihydroxy-1-(1-oxo-1H-isochromen-3-yl)butan-2-yl]oxy}-3,4,5-trihydroxyoxane-2-carboxylic acid	1.8246	1.8245	1.429	0.0005919	0.04157
pos_8602	Imidazoleacetic acid riboside	1.8146	1.8014	1.3558	0.0456	0.2386
neg_4719	PG(16:0/0:0)[U]	1.7958	1.7955	0.7417	0.01438	0.09671
pos_1892	Glutamylthreonine	1.7813	1.7722	0.7852	0.03446	0.2052
pos_6937	1H-Indole-3-acetamide	1.7578	1.7492	0.7386	0.03168	0.1978
pos_6162	6-(Allylthio)purine	1.7289	1.7196	0.7927	0.009898	0.1769
pos_8500	2,6-Piperidinedicarboxylic acid	1.7112	1.7035	0.7912	0.04079	0.2248
pos_3393	6-{[3-(2,4-dihydroxyphenyl)propanoyl]oxy}-3,4,5-trihydroxyoxane-2-carboxylic acid	1.7061	1.6969	0.7991	0.04256	0.2298
neg_6665	3,4,5-trihydroxy-6-({11-methoxy-13-oxo-6,8,20-trioxapentacyclo[10.8.0.0^{2},^{9}.0^{3},^{7}.0^{14},^{19}]icosa-	1.7021	1.7019	1.3945	0.03196	0.1518

	1(12),2(9),10,14(19),15,17-hexaen-15-yl}oxy)oxane-2-carboxylic acid					
neg_2875	Tyrosyl-Proline	1.6999	1.6999	0.7112	0.02832	0.1418
neg_5918	11Z-Eicosenoic acid	1.6886	1.6886	0.7376	0.03338	0.1552
neg_7629	Gamma-Glutamylphenylalanine	1.6696	1.6695	0.6878	0.005823	0.05985
pos_6881	5-Methoxyindoleacetate	1.669	1.659	1.361	0.003532	0.1184
neg_4782	Gamma-Eudesmol rhamnoside	1.6373	1.6371	0.7242	0.006739	0.06432
pos_6766	N1-(alpha-D-ribosyl)-5,6-dimethyl-benzimidazole	1.635	1.6273	1.2619	0.01152	0.1886
neg_3708	3-Hydroxyquinine	1.621	1.6206	0.7149	0.03991	0.1708
neg_6046	PE(15:1/0:0)	1.6184	1.6183	0.7839	0.007632	0.06951
neg_6910	Polyethylene, oxidized	1.6013	1.6012	1.384	0.009025	0.07568
pos_3761	Monotropein	1.5873	1.5784	0.7756	0.0004051	0.05312
neg_394	1,4-beta-D-Glucan	1.5865	1.5865	1.3184	0.00937	0.07703
neg_8440	Xanthopterin	1.5772	1.5772	0.6824	0.0396	0.1703
neg_4727	13,14-Dihydro-15-keto-PGE2	1.5385	1.5384	0.7996	0.02618	0.1353
pos_5977	Monic acid	1.5343	1.5256	0.8063	0.02313	0.1978
neg_7164	Indolelactic acid	1.4942	1.4941	0.6869	0.001609	0.04901
neg_179	N-Acetylneuraminic acid	1.4734	1.473	1.2493	0.04673	0.1856
neg_3095	Gamma-Glutamyltyrosine	1.4062	1.406	0.7945	0.009307	0.07669
neg_6254	3b-Hydroxy-6b-methoxy-7(11)-eremophilen-12,8a-olide	1.3024	1.3024	0.7853	0.04048	0.1721
neg_9042	Beta-Hydroxypyruvic acid	1.2473	1.2473	0.8255	0.01423	0.09635
pos_3287	4-Hydroxytacrine	1.1643	1.1572	0.8299	0.008418	0.1682

Table S10. The variable importance in the projection (VIP), Fold change (FC), *p-value*, and false discovery rate (FDR) value in metabolites abundance of UV-XJW48. The FC > 1.2 and $p < 0.05$ or FC < 0.83 and $p < 0.05$ were considered to indicate significantly upregulated and downregulated metabolites, respectively.

Mode ID	Metabolite	VIP (OPLS-DA)	VIP (PLS-DA)	FC	P_value	FDR
pos_2802	(15a,20R)-Dihydroxypregn-4-en-3-one 20-[glucosyl-(1->4)-6-acetyl-glucoside]	3.6716	3.5279	21.3557	0.005352	0.2663
neg_6907	2-{[hydroxy(4-methoxy-1-benzofuran-5-yl)methylidene]amino}acetic acid	3.1104	3.0205	0.1723	0.0002382	0.04135
pos_7644	PELLETIERINE	2.4514	2.3251	1.6155	0.013	0.3307
neg_3278	(6-carboxy-3,4,5-trihydroxyoxan-2-yl)[2-(3,4-dihydroxyphenyl)-3,5,6-trihydroxy-7H-chromen-7-ylidene]oxidanium	2.3936	2.3289	1.807	0.003042	0.05891
pos_8602	Imidazoleacetic acid riboside	2.3273	2.235	1.5111	0.02101	0.3923
neg_590	2-{2,6-dihydroxy-4-[6-hydroxy-7-(3-methylbut-2-en-1-yl)-1-benzofuran-2-yl]-3-methoxyphenyl}-6-(2,4-dihydroxyphenyl)-4-methylcyclohex-3-ene-1-carboxylic acid	2.3185	2.256	1.5511	0.004635	0.07879
pos_7036	Isoleucylproline	2.3134	2.2234	1.5342	0.009757	0.324
neg_5348	LysoPA(0:0/18:1(9Z))	2.2489	2.1974	0.634	0.0009392	0.04135
neg_7750	Chlorogenoquinone	2.2466	2.1858	1.5951	0.00026	0.04135
neg_3893	Butyl (S)-3-hydroxybutyrate glucoside	2.2317	2.1909	0.6178	0.003899	0.07025
pos_7882	Pyridine N-oxide glucuronide	2.2049	2.067	1.5244	0.04261	0.4769

neg_6891	5'-Deoxy-5-fluorouridine	2.1985	2.1462	0.6237	0.0005799	0.04135
neg_7164	Indolelactic acid	2.1137	2.0659	1.5156	0.01652	0.1766
pos_6460	5-Hydroxysulfamethoxazole	2.09	2.0841	0.6927	0.04014	0.4699
neg_397	3-Deoxy-D-glycero-D-galacto-2-nonulosonic acid	2.0476	1.9633	1.2891	0.01704	0.1807
neg_4719	PG(16:0/0:0)[U]	2.0304	1.9594	0.7336	0.004713	0.07972
neg_3966	6-[(5-{[2,2-dimethyl-7-(2-methylbut-3-en-2-yl)-5-[(2-methylbut-3-en-2-yl)oxy]-8-oxo-2H,8H-pyrano[3,2-g]chromen-10-yl]oxy}-2-methyl-7,10-bis(2-methylbut-3-en-2-yl)-8-oxo-2H,8H-pyrano[3,2-g]chromen-2-yl)methoxy]-3,4,5-trihydroxyoxane-2-carboxylic acid	1.9192	1.8693	1.3503	0.04513	0.2905
neg_3047	3,4,5-trihydroxy-6-{[7-methoxy-3-(3-methoxyphenyl)-8-methyl-4-oxo-4H-chromen-5-yl]oxy}oxane-2-carboxylic acid	1.9023	1.8518	1.3571	0.006372	0.09795
neg_391	1-Methylinosine	1.8743	1.8202	1.2712	0.02166	0.205
pos_6648	Coutaric acid	1.81	1.7104	1.2754	0.01777	0.3655
neg_7617	Gamma-Glutamylhistidine	1.7319	1.6848	1.3357	0.001513	0.04135
neg_4782	Gamma-Eudesmol rhamnoside	1.7118	1.6488	0.7539	0.008787	0.1192
neg_7161	3-(4-hydroxyphenyl)-N-(4-oxobutyl)prop-2-enimidic acid	1.7054	1.6293	1.3338	0.04152	0.2811
pos_6705	Ornithine	1.6428	1.5763	1.278	0.002615	0.2183
neg_8407	4-Pyridoxic acid	1.5878	1.5292	1.2549	0.01837	0.1866

pos_3761	Monotropein	1.5694	1.5133	0.8007	0.001354	0.2087
pos_649	(S)-ACPA	1.5651	1.5329	0.7876	0.04716	0.4903
pos_6631	4-AMINOETHYLBENZENESULFONYL FLUORIDE	1.5563	1.4834	0.812	0.007252	0.2923
pos_6766	N1-(alpha-D-ribosyl)-5,6-dimethyl-benzimidazole	1.542	1.4781	1.2079	0.004191	0.242
pos_7213	2-Ethylisonicotinamide	1.5273	1.5217	1.2245	0.03968	0.4694
pos_8202	5,7-dihydroxy-2-phenyl-8-(3,4,5-trihydroxyoxan-2-yl)-4H-chromen-4-one	1.461	1.3906	1.2069	0.03167	0.4417
neg_2014	D-Erythrose 4-phosphate	1.4297	1.3908	1.2051	0.00009565	0.03128

Table S11. The variable importance in the projection (VIP), Fold change (FC), *p-value*, and false discovery rate (FDR) value in metabolites abundance of GOUV-XJW48. The FC > 1.2 and $p < 0.05$ or FC < 0.83 and $p < 0.05$ were considered to indicate significantly upregulated and downregulated metabolites, respectively.

Mode ID	Metabolite	VIP (OPLS-DA)	VIP (PLS-DA)	FC	P_value	FDR
pos_2802	(15a,20R)-Dihydroxypregn-4-en-3-one 20-[glucosyl-(1->4)-6-acetyl-glucoside]	3.8559	3.8623	24.0626	0.01241	0.2062
neg_6907	2-{[hydroxy(4-methoxy-1-benzofuran-5-yl)methylidene]amino}acetic acid	2.8417	2.8349	0.1562	0.0002326	0.02144
neg_7660	Seryltryptophan	2.7607	2.7526	0	0.02104	0.1253
neg_3278	(6-carboxy-3,4,5-trihydroxyoxan-2-yl)[2-(3,4-dihydroxyphenyl)-3,5,6-trihydroxy-7H-chromen-7-ylidene]oxidanium	2.6471	2.6395	2.2083	0.001571	0.05119
pos_7644	PELLETIERINE	2.587	2.5834	1.698	0.009678	0.1847
pos_8898	1,3-Propanediamine	2.49	2.4963	1.7847	0.02261	0.2523
pos_3664	(S)-10,16-Dihydroxyhexadecanoic acid	2.4352	2.4387	1.5628	0.01034	0.1908
pos_3239	3R-aminononanoic acid	2.3559	2.3537	0.5963	0.0001762	0.08115
pos_904	Lumichrome	2.3369	2.3333	0.6369	0.02382	0.2588
neg_179	N-Acetylneuraminic acid	2.3177	2.3113	1.5886	0.001936	0.05417
neg_1774	L-Aspartic Acid	2.2842	2.2734	0.5661	0.03783	0.1698
pos_6162	6-(Allylthio)purine	2.2025	2.2061	0.6887	0.01731	0.2332
pos_3303	Diacetone alcohol	2.1983	2.1948	1.4771	0.002189	0.1151
pos_5791	Tangeritin	2.1752	2.1745	0.7152	0.03038	0.2795
pos_6248	(+)-4,11-Eudesmadien-3-one	2.1514	2.1526	1.4972	0.003268	0.1299

pos_6460	5-Hydroxysulfamethoxazole	2.1487	2.145	0.6803	0.03725	0.3055
pos_6623	Cucurbic acid	2.0931	2.0828	1.4612	0.04263	0.3188
neg_4371	Corchorifatty acid A	2.0836	2.0778	0.5952	0.004259	0.05656
neg_3893	Butyl (S)-3-hydroxybutyrate glucoside	2.0731	2.0674	0.6006	0.00359	0.05656
pos_6936	5-Hydroxy-L-tryptophan	2.0685	2.0663	0.6609	0.000629	0.08326
pos_3542	(1R*,2R*,4R*,8S*)-p-Menthane-1,2,8,9-tetrol 9-glucoside	2.0568	2.0558	0.707	0.001955	0.1145
neg_6891	5'-Deoxy-5-fluorouridine	2.0396	2.0343	0.6059	0.000549	0.03565
pos_6043	MG(15:0/0:0/0:0)	2.0253	2.0312	1.3774	0.02835	0.2795
neg_394	1,4-beta-D-Glucan	2.0112	2.007	1.5076	0.001085	0.04594
pos_8602	Imidazoleacetic acid riboside	1.9933	1.9871	1.38	0.01487	0.2207
pos_5941	3-(Hydroxymethyl)-2-octanone	1.9597	1.9648	1.2876	0.02349	0.2566
neg_7153	3,4,5-trihydroxy-6-(2-methyl-3-phenylpropoxy)oxane-2-carboxylic acid	1.9166	1.9089	1.5306	0.02908	0.1479
pos_3274	Aloe emodin anthrone	1.8592	1.857	1.3094	0.0008739	0.0858
neg_397	3-Deoxy-D-glycero-D-galacto-2-nonulosonic acid	1.8345	1.8319	1.2877	0.01553	0.1073
neg_4372	13,14-dihydro-15(R)-Prostaglandin E1	1.8036	1.7989	0.7305	0.0003012	0.02489
pos_5776	1alpha-hydroxyvitamin D3	1.7987	1.7983	0.7481	0.01916	0.2422
pos_6705	Ornithine	1.7939	1.7854	1.3423	0.04052	0.3135
pos_6631	4-AMINOETHYLBENZENESULFONYL FLUORIDE	1.7786	1.7793	0.7499	0.003498	0.1303
neg_6983	5-Phenyl-1,3-oxazinane-2,4-dione	1.7755	1.7748	0.7844	0.02677	0.1419
neg_391	1-Methylinosine	1.7507	1.7468	1.2874	0.0004456	0.03161
pos_3393	6-{[3-(2,4-	1.7493	1.7459	0.8065	0.04609	0.3309

	dihydroxyphenyl)propanoyl]oxy}-3,4,5-trihydroxyoxane-2-carboxylic acid					
pos_8202	5,7-dihydroxy-2-phenyl-8-(3,4,5-trihydroxyoxan-2-yl)-4H-chromen-4-one	1.743	1.7435	1.2878	0.007444	0.1693
neg_7136	6-{[1,3-dihydroxy-1-(1-oxo-1H-isochromen-3-yl)butan-2-yl]oxy}-3,4,5-trihydroxyoxane-2-carboxylic acid	1.7194	1.7127	1.3891	0.02511	0.1375
neg_7629	Gamma-Glutamylphenylalanine	1.7011	1.6965	0.6772	0.002209	0.05656
pos_7798	Glutamylphenylalanine	1.7002	1.701	1.3537	0.003015	0.1281
neg_6048	(-)-Arctigenin	1.6634	1.6601	1.3211	0.001592	0.0513
pos_3448	5-(3,4,5-trihydroxyphenyl)pentanoic acid	1.6601	1.6549	1.2299	0.01529	0.224
neg_1109	11(S)-HEPE	1.6531	1.6521	0.7865	0.03873	0.1719
neg_2875	Tyrosyl-Proline	1.6265	1.62	0.734	0.03794	0.1701
pos_3761	Monotropein	1.6223	1.6201	0.7859	0.001112	0.08787
neg_4782	Gamma-Eudesmol rhamnoside	1.6204	1.6171	0.7297	0.006991	0.07117
pos_7590	Pantothenol	1.6109	1.6095	1.3122	0.02726	0.2751
neg_4318	MG(0:0/18:3(6Z,9Z,12Z)/0:0)	1.5983	1.5969	0.763	0.02223	0.1289
pos_7395	4-Methylene-L-glutamine	1.5961	1.591	1.2198	0.01738	0.2332
pos_5977	Monic acid	1.5655	1.5625	0.8154	0.02607	0.2687
neg_8440	Xanthopterin	1.5624	1.5575	0.6887	0.04114	0.1764
neg_2257	S-Prenyl-L-cysteine	1.5573	1.5535	1.2855	0.00002422	0.01207
neg_590	2-{2,6-dihydroxy-4-[6-hydroxy-7-(3-methylbut-2-en-1-yl)-1-benzofuran-2-yl]-3-methoxyphenyl}-6-(2,4-	1.5472	1.5427	1.3005	0.002432	0.05656

	dihydroxyphenyl)-4-methylcyclohex-3-ene-1-carboxylic acid					
neg_4388	Myristoleic acid	1.5288	1.5296	0.7892	0.04938	0.1945
neg_9003	A-L-Arabinofuranosyl-(1->2)-[a-D-mannopyranosyl-(1->6)]-D-mannose	1.5277	1.5245	0.7584	0.01979	0.1219
pos_7601	5-Pyridoxolactone	1.5218	1.5188	1.2144	0.03494	0.2972
neg_6046	PE(15:1/0:0)	1.4584	1.4511	0.8184	0.04695	0.1892
neg_7617	Gamma-Glutamylhistidine	1.409	1.4077	1.277	0.01702	0.1127
neg_9122	ADP-ribose	1.3729	1.3711	0.7734	0.02838	0.1461
neg_6254	3b-Hydroxy-6b-methoxy-7(11)-eremophilen-12,8a-olide	1.2868	1.2827	0.7905	0.04251	0.1782